uniformity has been taken as evidence of operation of some type of natural selection. The present study revealed similar patterns of genic variation at nine polymorphic loci in two natural populations of *D. busckii* and this could be interpreted due to action of some type of natural selection (Tables 2–4). The present studies need to be extended to several ecogeographical populations of *D. busckii* to assess the extent of genetic variability in this species compared to the other colonizing *Drosophila* species.

1. Wills, C., *Genetic Variability*, Clarendon Press, Oxford, 1981.
2. Milkman, R., *Perspectives in Evolution*, Sinauer Associates, Inc., Champaign, 1982.
3. MacIntyre, R. J., *Molecular Evolutionary Genetics*, Plenum, New York, 1986.
4. Parkash, R., *Ind. Rev. Life Sci.*, 1987, **7**, 141.
5. Prakash, S., *Genetics*, 1973, **75**, 571.
6. Parsons, P. A., *Evol. Biol.*, 1980, **13**, 175.
7. Harris, H. and Hopkinson, D. A., *Handbook of Enzyme Electrophoresis in Human Genetics*, North-Holland, Amsterdam, 1976.
8. Dickinson, W. J. and Sullivan, D. T., *Gene Enzyme Systems in Drosophila*, Springer-Verlag, Berlin, 1975.
9. Fergusson, A., *Biochemical Systematics and Evolution*, Wiley, New York, 1980.
10. Zar, J. H., *Biostatistical Analysis*, Prentice-Hall, Englewood, New Jersey, 1984.
11. O'Brien, S. J. and MacIntyre, R. J., in *Genetics and Biology of Drosophila* (eds Ashburner, M. and Wright, T.), Academic Press, London, 1978, vol. 2a, p. 396.
12. Gillespie, J. H. and Kojima, K., *Proc. Natl. Acad. Sci. USA*, 1966, **61**, 582.
13. Johnson, G. B., *Science*, 1974, **184**, 28.
14. Hedrick, P. W., *Genetics of Populations*, Science Books International, Boston, 1983.
15. Karlin, S. and Nevo, E., *Evolutionary Processes and Theory*, Academic Press, New York, 1986.
16. Girard, P., Palabost, L. and Petit, C., *Biochem. Genet.*, 1977, **15**, 589.
17. Singh, R. S., Hickey, D. A. and David, J. R., *Genetics*, 1982, **101**, 235.

ACKNOWLEDGEMENTS. Financial assistance from CSIR, New Delhi, is gratefully acknowledged. J. P. Yadav thanks UGC, New Delhi for a fellowship. We are grateful to the reviewer for several helpful suggestions.

21 March 1989; revised 15 November 1989

Gasket-compression mechanism of pressure-pulse generation by low-velocity projectile impact on opposed anvil set-up

A. K. Singh
Materials Science Division, National Aeronautical Laboratory, Bangalore 560 017, India

High pressure pulse is generated when a low-velocity projectile strikes a tungsten carbide opposed anvil system with pyrophyllite gasket and solid pressure transmitting medium. A possible mechanism based on the gasket-compression is proposed for generation of such pressure pulses.

IT has been shown recently[1] that a high pressure pulse of short duration is produced in the gasket region when a low-velocity projectile strikes a tungsten carbide-opposed anvil set-up with pyrophyllite gasket and solid pressure transmitting medium. Both the amplitude and the duration of the pressure pulse depend upon the momentum of the projectile. The experiments with anvils of 12 mm diameter face indicate that the amplitude of the pressure pulse increases from 2 to 6 GPa and the pulse duration from 280 to 380 μs as the momentum of the projectile (mass in the range of 5–10 kg) is increased from 10 to 60 kg m s^{-1}.

The pressure versus time data representing a typical pressure pulse as derived from the resistance-time data of a manganin gauge, are shown in Figure 1. Except in the small regions near the start and the peak of the pressure pulse, the pressure is found to increase linearly with time, the nonlinearity being $<5\%$. The rate of pressure increase can be varied between 0.03 and

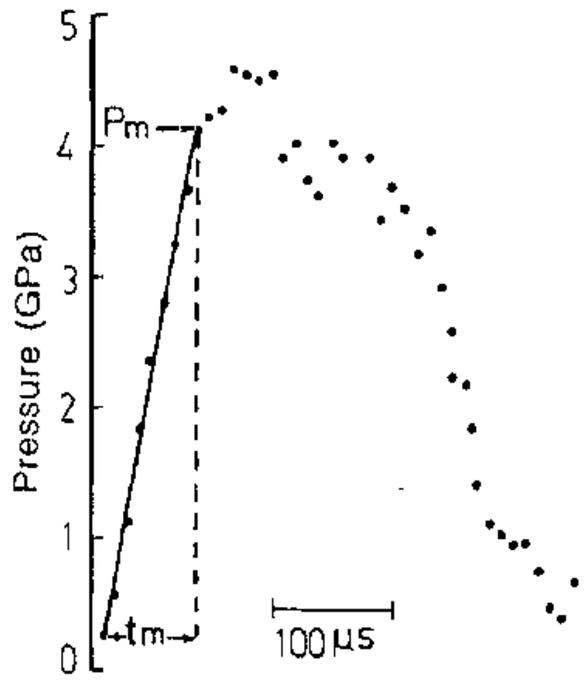

Figure 1. A typical pressure pulse obtained under impact loading. P_m is the maximum pressure up to which the pressure increase is linear. The peak pressure is 10–15% higher than P_m.

0.1 GPa $(\mu s)^{-1}$ by varying the momentum of the projectile between 10 and 60 kg m s^{-1}.

During the impact, the projectile dissipates its kinetic energy mainly by two processes, viz. compression of the gasket and generation of elastic waves which propagate through the entire assembly of push-rod, anvils and the platens. The small fraction of the projectile energy which appears as audible sound energy may be neglected. The transfer of projectile momentum to the anvils is prevented as the lower anvil is backed by a massive platen (weighing ~300 kg).

The plastic compression of the gasket during impact plays an important role in the generation of pressure pulses. Under the impact of the projectile, the gasket flows radially and gets compressed axially, resulting in the force responsible for decelerating the projectile on impact. If the fraction of the projectile energy propagating as elastic waves in the anvils and the press is assumed to be small, then the instantaneous pressure, $P(t)$ at the centre of the gasket is related to the rate of change of momentum of the projectile as follows,

$$P(t) = -(K/A)\, \mathrm{d}(mv)/\mathrm{d}t, \qquad (1)$$

where m and v denote respectively the mass and the velocity of the projectile, and A the area of the anvil face. A consideration[2,3] of the various forces acting on a gasket under static compression indicates that stress distribution is symmetric about the anvil axis and varies radially, peaking at the centre of the gasket. The radial stress gradient in the central region of the gasket (where the sample is located) is reduced by the use of solid pressure-transmitting medium. The pressure at the centre still differs from the nominal pressure calculated by simply dividing the force on the anvil by the anvil face area. The factor K is the ratio of the actual pressure at the centre of the gasket to the nominal pressure. The static pressure experiments indicate that $K \approx 2.5$ for the dimensions of the gaskets used in the present experiments. Further, K is found to remain nearly constant up to 7.5 GPa. On integrating both sides of equation (1) in the time interval wherein the pressure increase is linear, we get,

$$P_m = (2K/At_m)\,(fmv_0). \qquad (2)$$

The terms P_m and t_m are indicated in Figure 1, and f is a fraction (<1). The term fmv_0 simply represents the change in momentum of the projectile, expressed as a fraction of the initial momentum, during time interval t_m.

The continuous line in Figure 2 represents the best fit through the P_m versus momentum data obtained in a large number of experiments. The value of P_m increases linearly with projectile momentum initially, and flattens out at higher momenta. It appears that the fraction of the projectile energy transmitted through the anvils as stress waves increases with increasing momentum and

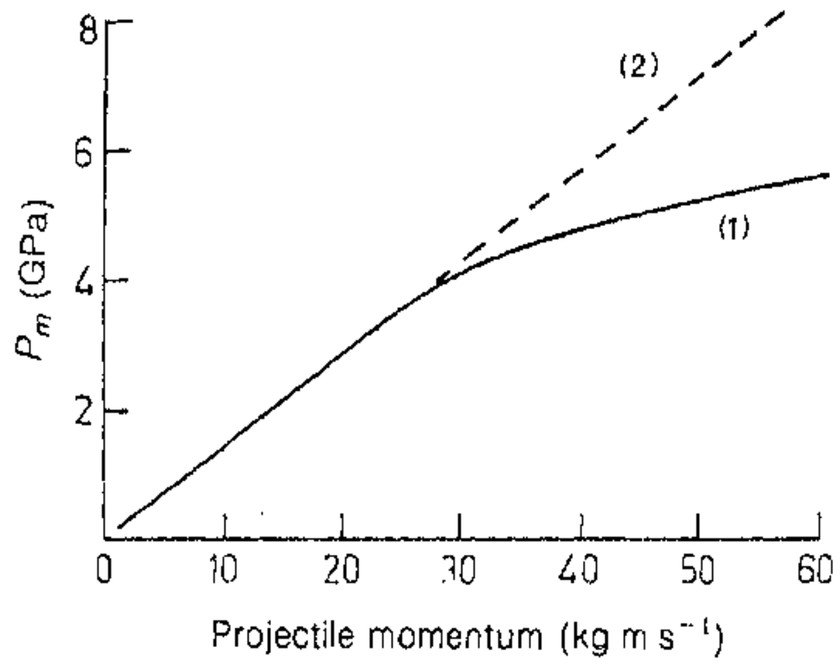

Figure 2. P_m as a function of projectile momentum. Best fit through experimental data (1), and calculated values (2).

consequently P_m ceases to be proportional to the initial momentum of the projectile. The dashed line represents the best fit through the values of P_m calculated from (2) using the experimental values of t_m and mv_0, and the appropriate values of K and A. Because of the practical difficulty in determining K under the impact loading, the measured value under static load has been used in calculating P_m. The possibility of K being different under impact loading and static loading for the same gasket dimensions cannot be ruled out; the difference, however, is unlikely to be so large as to invalidate the present discussion. The best fit between the observed and the calculated values of P_m in the 10–30 kg m s^{-1} momentum range is obtained with $f = 0.5$. This means that the projectile loses about half its momentum by the time the pressure reaches P_m. The calculated value of P_m at higher momenta is consistently higher than the corresponding observed value, the difference between the two increasing with increasing momentum. This trend again suggests that as the projectile momentum increases, an increasingly larger fraction of the projectile energy is lost as elastic waves propagating through the anvils and the press.

The gasket flow decreases with increasing static pressure and ceases at ~8 GPa, beyond which the compression becomes predominantly elastic[2,3]. The cessation of the gasket flow results in a significant drop in K. This means that a given increase in pressure in the region of elastic compression requires a much larger increase in the applied load than if the gasket underwent plastic compression. If a similar behaviour of the gasket is assumed under impact load, then initially under impact the gasket flows and the projectile energy is dissipated in compressing the gasket. Because of the compression, the pressure is generated selectively in the gasket region. In the 10–30 kg m s^{-1} momentum range (Figure 2), this mechanism seems to be operative. When the experiments are done with still higher projectile momentum, pressure is

generated initially by the mechanism of gasket compression. As the pressure increases, further flow of the gasket decreases, and the energy of the projectile is dissipated by the appearance of elastic waves in the anvils and the press.

1. Singh, A. K., *Rev. Sci. Instrum.*, 1989, **60**, 253.
2. Okai, B. and Yoshimoto, J., *High Temp-High Pressures*, 1973, **5**, 675.
3. Prins, J. F., *High Temp-High Pressures*, 1983, **15**, 21.

22 September 1989

Consequences of predicted sea level rise for the Lakshadweep islands

M. C. Pathak and K. L. Kotnala
National Institute of Oceanography, Dona Paula, Goa 403 004, India

The impact of accelerated sea level rise on coastal regions and islands and the ability to adopt to environmental changes of a particular shoreline depend on local topographic characteristics. The Lakshadweep islands off the south-west coast of India, with a maximum height of 4 m above present mean sea level, may be particularly vulnerable to the consequences of sea level rise due to the greenhouse effect. Available data on the topography of Kiltan, Kavaratti, Kadmat, Kalpeni–Cheriyam and Agatti–Bangaram islands suggest that the predicted sea level rise scenario value of 1 m may be responsible for 19, 11, 19, 21 and 18% land loss in these islands.

THERE are indications to believe that due to an increase in the concentration of greenhouse gases in the atmosphere[1], the global mean surface temperature and the sea level have risen and are expected to continue to rise. Even though there are considerable uncertainties in estimating the future sea level rise, due to its non-uniformity over the globe[2] it will be prudent at this stage to examine the consequences of accelerated sea level rise for the low-lying areas of the Indian coast. The dominant effects of accelerated sea level rise on the coastal region will be: (a) submergence of extensive low-lying areas, posing a serious threat to the coastal population and to the ecology of the region, (b) damages due to an increase in storm surges, (c) possible salt water intrusion into coastal freshwater aquifers, etc. Vulnerability study of Indian coastal region for sea level changes due to the greenhouse effect[3, 4] indicates that the low-lying coral islands of the Lakshadweep archipelago are the most sensitive. The projected scenario of 1 m rise[5, 6] in sea level on these islands, with a maximum height of 4 m above the present sea level will certainly effect the morphology and restrict the human activities on these islands. Moreover, small islands rising from the deep oceanfloor provide the best sites for measuring a sea level rise[7] and could provide useful data for sea level studies. Hence, a few islands (Kiltan, Kavaratti, Kadmat, Kalpeni–Cheriyam and Agatti–Bangaram) from this group were selected for a pilot study (Figure 1).

Recurring changes in the shoreline position in the past and visualizing the impact of the anticipated sea level change could be studied by comparing the paleo-shoreline maps with the present shoreline map[4]. This procedure is used for the present study with the echograms of the surrounding areas of the islands.

An examination of the echograms of the Kiltan, Kavaratti, Kadmat, Kalpeni–Cheriyam, and Agatti–Bangaram Islands of Lakshadweep has revealed the occurrence of marine terraces (submerged shore) at 7–12, 15, 21–36 and 50 m of water depth[8]. In the absence of information on the particular age of these terraces the age of 9135 years B.P. for the nearby composite shells from the sediments at 58 m water depth[9] has been assumed for the 50 m terrace, which almost corresponds to the calculated mean age from the eustatic curves. Use of the above method indicates that the effect of sea level rise accounts for about 76, 71, 91, 92 and 96% of the total horizontal land loss at the rates of 7.4, 9.9, 18.1, 28.5 and 32.6 cm per year respectively for Kiltan, Kavaratti, Kadmat, Kalpeni–Cheriyam and Agatti–Bangaram Islands (Table 1, Figure 2*a*).

Gornitz has estimated a 10–15 cm global sea level rise during the last century[10]. Hoffman[5] has summarized the predicted values of sea level rise for the years 2000 to 2100 years for different scenario (Table 2), which shows that by the year 2050, the magnitude of the sea

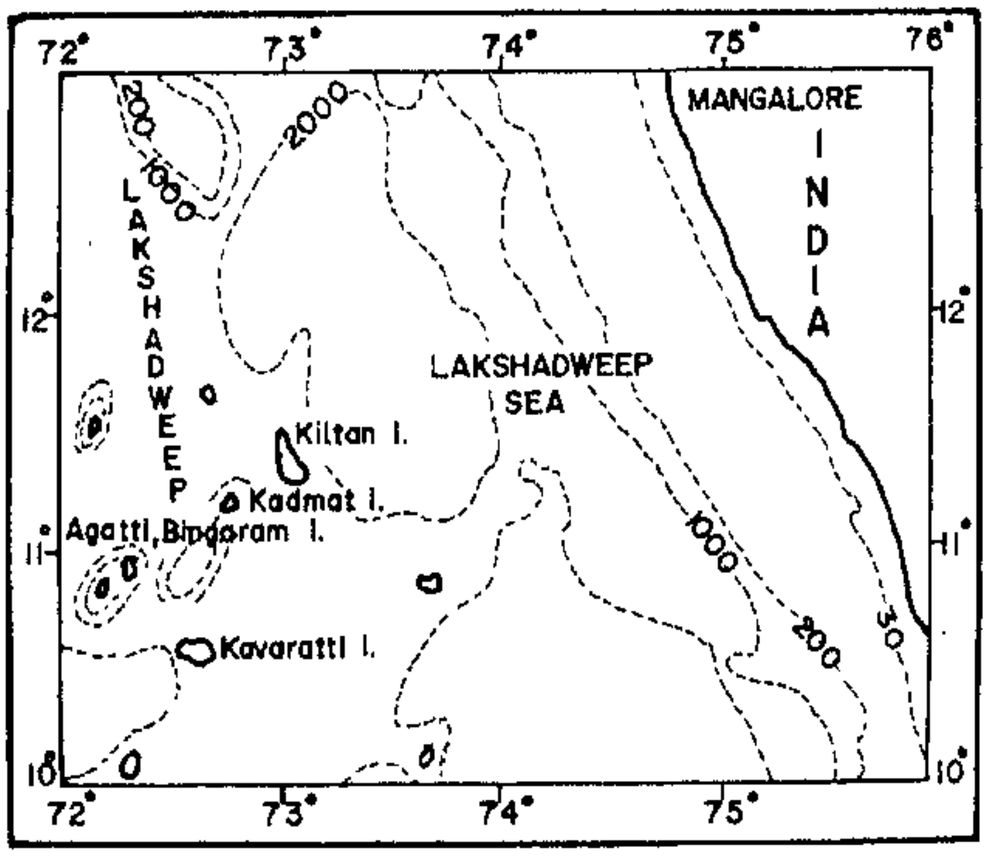

Figure 1. Map showing location of Lakshadweep Islands.